Applied Physics Letters ARTICLE scitation.org/journal/apl

Multiferroic $LuFeO_3$ on GaN by molecular-beam epitaxy

Cite as: Appl. Phys. Lett. **116**, 102901 (2020); doi: 10.1063/1.5143322
Submitted: 21 December 2019 · Accepted: 27 February 2020 ·
Published Online: 10 March 2020

View Online Export Citation CrossMark

Joseph Casamento,[1,a)] Megan E. Holtz,[1] Hanjong Paik,[1,2] Phillip Dang,[3] Rachel Steinhardt,[1] Huili (Grace) Xing,[1,4,5] Darrell G. Schlom,[1,5] and Debdeep Jena[1,4,5]

AFFILIATIONS

[1]Department of Materials Science and Engineering, Cornell University, Ithaca, New York 14853, USA
[2]Platform for the Accelerated Realization, Analysis, and Discovery of Interface Materials (PARADIM), Cornell University, Ithaca, New York 14853-1501, USA
[3]School of Applied and Engineering Physics, Cornell University, Ithaca, New York 14853, USA
[4]School of Electrical and Computer Engineering, Cornell University, Ithaca, New York 14853, USA
[5]Kavli Institute at Cornell for Nanoscale Science, Cornell University, Ithaca, New York 14853, USA

[a)]Author to whom correspondence should be addressed: jac694@cornell.edu

ABSTRACT

Hexagonal $LuFeO_3$ exhibiting ferroelectricity and weak ferromagnetism is grown on metal-polar GaN by molecular-beam epitaxy. The oxide films exhibit smooth surface morphologies and are found to be single crystalline with an epitaxial relationship related by a 30° in-plane rotation relative to the GaN crystal structure. The $LuFeO_3$ layers grown on GaN exhibit room-temperature ferroelectricity and low-temperature magnetic ordering. This epitaxial integration creates a heterostructure platform to explore and exploit the coupling of the ferroelectricity and magnetism of oxides with the strong spontaneous and piezoelectric polarization and the unique electronic and photonic properties of nitride semiconductors.

Published under license by AIP Publishing. https://doi.org/10.1063/1.5143322

Oxide crystals demonstrate a rich range of physical phenomena such as piezoelectricity, ferroelectricity, multiferroicity, colossal magnetoresistance, superconductivity, and metal/insulator transitions.[1,2] The polar nitride crystals, GaN, AlN, and InN, and their corresponding semiconducting alloys exhibit strong spontaneous and piezoelectric polarization and have now become a platform for high-performance optical and electronic devices. Epitaxially combining oxides and nitrides can offer unique dielectric heterostructures to enable, for example, ferroelectric gate transistors with applications in RF communications, low-power logic, and integrated memories.[3,4]

Significant advances have occurred in the understanding of non-epitaxial (e.g., atomic-layer deposited) ferroelectric/non-polar semiconductors, for example, HfZrO–Si structures[5] and the effect of defects on their properties. Although epitaxial heterostructures offer the possibility of controlling chemical and electronic defects, efforts to integrate such structures lag far behind. Previous efforts include the growth of epitaxial ferroelectrics such as $Pb(Zr,Ti)O_3$ and multiferroics such as $YMnO_3$ and $BiFeO_3$ on GaN by sputtering and by oxide molecular-beam epitaxy (MBE).[6–11] For example, growing $BiFeO_3$, a known room-temperature multiferroic, epitaxially on GaN necessitates buffer layers and results in twin-domains.[11] $LuFeO_3$ is a weaker ferroelectric than $BiFeO_3$: for example, its lower ferroelectric polarization of $\sim 5\ \mu C/cm^2$ (compared to $\sim 100\ \mu C/cm^2$ of $BiFeO_3$) is better matched to typical polarization-induced two-dimensional electron gas densities seen in nitride heterostructures.

In this work, we present the epitaxial growth of $LuFeO_3$ on the (0001) surface of metal polar GaN. Bulk $LuFeO_3$ has an orthorhombic crystal structure and is not ferroelectric. As a thin film, $LuFeO_3$ can be epitaxially stabilized with a hexagonal crystal structure,[12] making it appealing for integration with hexagonal III-nitride semiconductors. $LuFeO_3$ offers a viable path toward room-temperature multiferroicity.[13] Thin-film hexagonal $LuFeO_3$ is a geometric ferroelectric with a Curie temperature of $T_C \sim 1020$ K;[14] the polarization dipoles are formed by the broken inversion symmetry in the ordering of Lu atoms. Due to its improper ferroelectricity, where spontaneous polarization is not the primary order parameter, $LuFeO_3$ is expected to retain its ferroelectric properties down to two unit cells.[15] Such scalability to nanoscale dimensions is fundamentally interesting for high-density logic and memory applications. Owing to interacting spins of the Fe sublattice, $LuFeO_3$ also shows canted antiferromagnetic ordering below 147 K,[14,16,17]

Published under license by AIP Publishing

making it a low-temperature multiferroic. This multiferroic coupling can be tuned near room temperature by forming superlattices with ferrimagnetic $LuFe_2O_4$ layers.[13] Accordingly, epitaxial $LuFeO_3$ and $LuFeO_3$-based superlattices present an exciting opportunity for integration with the nitride family, which itself is currently expanding into magnetic, superconducting, and ferroelectric research domains.[18]

The oxide MBE growth in this study was performed using a Veeco® GEN10 system. KSA Instruments reflection high-energy electron diffraction (RHEED) apparatus with a Staib electron gun operating at 14 kV and 1.4 A was used for *in situ* monitoring of film growth. After growths, the film orientation was characterized using a Rigaku SmartLab x-ray diffraction (XRD) and a PANalytical X'Pert Pro setup at 45 kV, 40 mA with Cu $K\alpha_1$ radiation (1.54057 Å). Piezoresponse force microscopy (PFM) measurements were performed using an Asylum Research Cypher ES AFM system with conductive Nanosensors PointProbe Plus (PPP)-Electrostatic Force Microscopy (EFM) tips to apply bias to the sample surface.

$LuFeO_3$ thin films of ~30 nm thickness were deposited on 10 mm × 10 mm (0001)-oriented Ga-polar GaN/Al_2O_3 template substrates in an ozone MBE system. Before growth, GaN/Al_2O_3 template substrates were cleaned in acetone, isopropyl alcohol, methanol, and hydrochloric acid (HCl). High purity (99.99%) elemental Lu and Fe were supplied from effusion cells at fluxes of $\sim 1.5 \times 10^{13}$ atoms/cm^2 s. A mixture of oxygen and ~10% ozone at a background partial pressure of 10^{-6} Torr was supplied. Three growth temperatures: 700, 800, and 900 °C (as measured by the substrate heater thermocouple) were investigated. Figures 1(a)–1(c) show the *in situ* RHEED patterns of the $LuFeO_3$ after growth at the three temperatures. For samples grown at 700 °C and 900 °C, the RHEED streaks broaden and lose intensity relative to those grown at 800 °C. The sample grown at 800 °C shows a sharp streak pattern, indicating the epitaxial nature of the $LuFeO_3$ epilayer. The RHEED pattern for growth at 700 °C is broad and an almost diffuse streak, potentially due to low surface adatom mobility at this lower temperature. Figures 1(d) and 1(e) show the corresponding AFM images of samples grown at 800 °C and 900 °C. The surface morphologies are smooth, with RMS of 1.5 nm for 10 μm × 10 μm scans for the 800 °C sample. The higher roughness for samples grown at 700 °C (1.9 nm, not shown) and 900 °C (1.8 nm) is related to their deviation from an optimal growth temperature. No indication of additional phases or Fe_3O_4 precipitates that were reported in Ref. 17 are

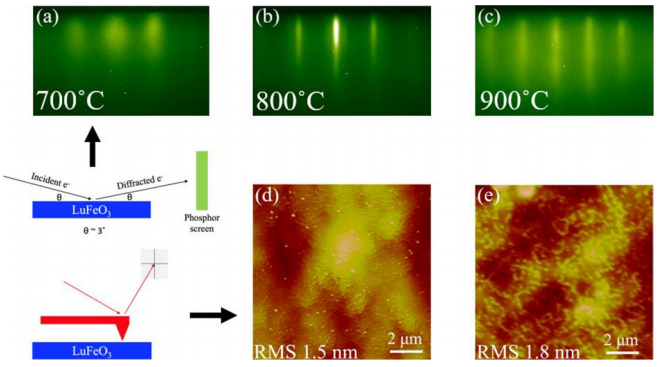

FIG. 1. RHEED images post-growth along ⟨11$\bar{2}$0⟩ azimuth at substrate temperatures of 700 °C, 800 °C, and 900 °C with schematic underneath. Corresponding AFM images with schematic on left for growths at 900 °C (e) and 800 °C (d), with a coarser morphology seen for growths at 900 °C.

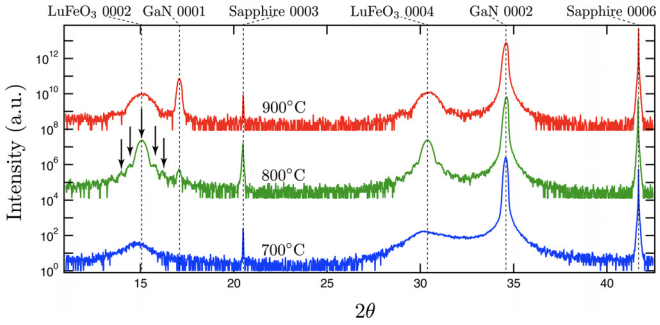

FIG. 2. XRD Θ-2Θ scans for $LuFeO_3$ epitaxial layers grown on GaN-Al_2O_3 substrates at temperatures of 700, 800, and 900 °C. The arrows for the 800 °C sample indicate the thickness fringes.

seen. $LuFeO_3$ can tolerate non-stoichiometry in the form of excess and/or deficient Lu or Fe and still appear phase pure by XRD.[17]

XRD symmetric Θ-2Θ scans are shown in Fig. 2 for $LuFeO_3$ grown at the three temperatures. The presence of 0002 and 0004 peaks of $LuFeO_3$ indicates that all as-grown thin films are hexagonal. The highest film quality is seen for the sample grown at 800 °C; it has a more intense 0002 peak compared to those grown at 700 and 900 °C. Furthermore, this sample exhibits fully developed thickness fringes. A clear 0002 peak is seen for films grown at 700 °C, but the film quality may be reduced at that temperature due to insufficient mobility of adatoms on the surface. Film quality may be reduced for growth at 900 °C due to thermal decomposition of GaN prior to deposition although no direct evidence of this was seen as the substrate was heated up quickly at a ramp rate 150 °C/min to 900 °C and no change in RHEED was observed before the growth started. The GaN and sapphire peaks are visible: the XRD peak seen near $2\Theta = 17.1°$ matches that for a GaN 0001 peak[19] and no impurity phases related to excess Fe or Lu are evident. The obtained $LuFeO_3$ lattice parameters for films grown at 800 and 900 °C were $a = 5.979$ Å and $c = 11.81$ Å ± 0.001 Å.

To determine the epitaxial relationship of $LuFeO_3$ and GaN, off-axis phi (ϕ) scans were performed on asymmetric GaN 10$\bar{1}$6 and $LuFeO_3$ 10$\bar{1}$4 peaks for the sample grown at 800 °C. The ϕ scans shown in Fig. 3 indicate sixfold symmetry for both GaN and $LuFeO_3$, with the peaks offset by 30° relative to each other. This is indicative of a 30° in-plane rotation of the $LuFeO_3$ with respect to the underlying

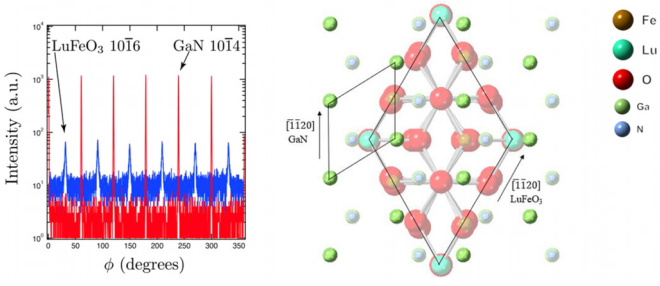

FIG. 3. Left: XRD phi (ϕ) scans showing the sixfold symmetry of $LuFeO_3$ and GaN, with a 30° offset indicating a 30° in-plane rotation relationship. Right: CrystalMaker images of $LuFeO_3$ and GaN crystals looking down the c plane, with shown unit cells and [1$\bar{1}$20] directions to illustrate the 30° in-plane rotation.

Published under license by AIP Publishing

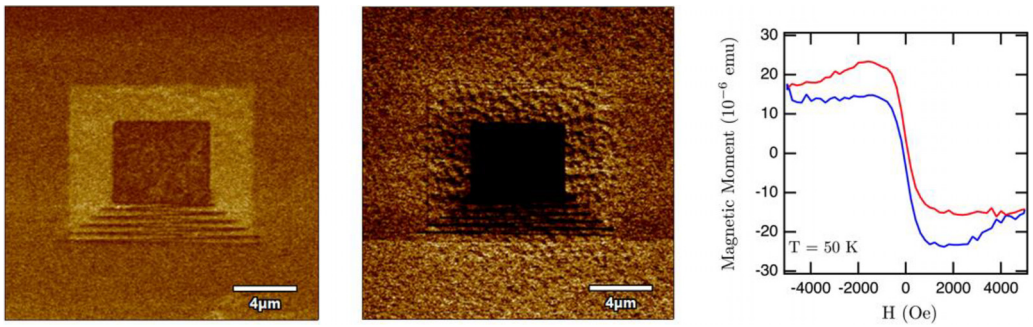

FIG. 4. PFM images of $LuFeO_3$-nGaN sample and VSM image of $LuFeO_3$-GaN. Left: piezoresponse channel (±5 V applied in smaller regions). Center: piezoresponse channel after 3 days, suggesting charge injection is not the mechanism for the pattern formation. Right: non-background subtracted VSM data showing hysteresis. The blue curve sweeps from negative to positive magnetic field, and the red curve sweeps from positive to negative magnetic field.

GaN. A similar epitaxial relationship has been seen previously[10] in a structural analog: $YMnO_3$ grown on GaN (0001). Because the GaN is metal-polar, oxygen atoms sit at "f.c.c" sites, namely, in the center of the threefold cavity between Ga and N atoms. Accordingly, the Ga–O chemical bond energetics leads to a similar 30° rotation in the $LuFeO_3$ layer stabilizing its hexagonal phase as indicated by the plan-view crystal structures shown in Fig. 3. This 30° in-plane rotation causes the lattice mismatch between $LuFeO_3$ and GaN to be ∼7.6%.

To test for ferroelectric behavior, ∼30 nm thick films of $LuFeO_3$ were grown on ∼150 nm thick *n*-type doped GaN with N_D ∼10^{19}/cm^3 Si donor doping. The underlying nGaN layers were grown in a separate plasma MBE system on the Si face of 6H-SiC substrates at a substrate temperature of 750 °C as measured by a thermocouple. The nGaN layer served as the bottom electrode for PFM measurements. Conductive Nanosensors PPP EFM tips were used to apply combined ac and dc biases to the bare $LuFeO_3$ surface to track contact resonance frequency and bias the sample, respectively. The contact resonance frequency was tracked during scanning using a dual ac resonance tracking (DART) mode. Contact to the underlying nGaN layer was made by applying silver paste along the edge of the sample to electrically ground it to an underlying metal disk. During the PFM measurements, positive and negative 5 V dc biases were applied in square regions on the sample. The bias was then removed and subsequent scans at 0 V dc biases were utilized to determine if the regions retained their poled state. In addition, the same region was observed three days later, suggesting the source of the pattern is not due to just electrostatics.

Figure 4 shows that a square pattern is formed by electrical poling. This is indicative of 180° polarization switching (e.g., up to down), which is expected for the symmetry allowed polarization directions of a hexagonal crystal. Retention and switching of polarization are the characteristics of a ferroelectric material. In the PFM scans, no significant phase contrast is seen before applying a dc bias, indicating the ferroelectric domain size in $LuFeO_3$ is likely much smaller than the ∼100 nm resolution of the current scans. From the PFM measurements, the coercive field for switching determined by the applied dc bias over the film thickness is estimated to be <2 MV/cm, much lower than the ∼3.8 MV/cm breakdown field of GaN.[20] At this stage, several properties of $LuFeO_3$ such as its permittivity and its band offsets with GaN are unknown, which prevents further quantitative analysis of the ferroelectricity in this heterostructure, but it will be the subject of subsequent studies.

Interacting spins of the Fe sublattice of the crystal are known to make hexagonal $LuFeO_3$ magnetic below a Néel temperature of ∼147 K.[17] The magnetic ground state of $LuFeO_3$ is stabilized by an A_2 spin configuration with 120° ordering of spins in-plane. There also exists spin canting, which causes a weak out-of-plane magnetic moment.[21] We investigated the $LuFeO_3$ films grown on GaN for magnetism by performing out-of-plane vibrating sample magnetometry (VSM) measurements on diced 3 mm × 3 mm samples. In VSM, a sample is oscillated about a magnetometer in a magnetic field and the generated AC voltage is proportional to the magnetic moment of the material. Although relatively weak magnetization strength is difficult to detect in VSM measurements of thin films (∼30 nm), Fig. 4 shows a hysteresis loop indicative of canted-antiferromagnetic behavior at 50 K, lower than the reported Néel temperature for $LuFeO_3$. Off-stoichiometric (e.g., Fe deficient) films have exhibited lower Néel temperatures in previous studies.[17] The out-of-plane magnetic moment of $LuFeO_3$ right below the Néel temperature is on the order of 0.005 μB/Fe atom. The magnetization increases as temperature decreases and reaches ∼0.02 μB/Fe atom around 50 K.[17] This is likely why VSM measurements at higher temperatures (e.g., 100 K, 150 K) were not able to clearly resolve the magnetization in our thin films. Nevertheless, weak ferromagnetism and ferroelectricity are confirmed in the epitaxial $LuFeO_3$ layer.

In conclusion, the epitaxial growth of the multiferroic $LuFeO_3$ is achieved on GaN. The resulting films are single crystalline with a 30° in-plane epitaxial relationship, as evidenced by *in situ* RHEED and post-growth XRD. Room-temperature PFM measurements suggest that $LuFeO_3$ grown on GaN (0001) is ferroelectric. In addition, the films show evidence of low-temperature canted-antiferromagnetic behavior. Future work will need to evaluate the permittivity and further ferroelectric properties of $LuFeO_3$ grown on GaN, the density of interface electronic states, its band offsets with the nitride semiconductors, and the coupling of its ferroelectric order parameter with the polarization of GaN in especially designed heterostructures. This will enable its integration with GaN based electronic and photonic devices.

This research was supported by National Science Foundation (NSF) Grant Nos. E2CDA 1740286 and NewLAW EFRI 1741694 and partially supported by the Semiconductor Research Corporation (SRC) as nCORE task 2758. H.P. was supported by the NSF [Platform for the Accelerated Realization, Analysis and Discovery of Interface Materials (PARADIM)] under Cooperative

Published under license by AIP Publishing

Agreement No. DMR-1539918. This work made use of the CNF, CCMR, and CESI Shared Facilities partly sponsored by the NSF NNCI program (No. ECCS-1542081), MRSEC program (No. DMR-1719875), MRI DMR-1338010, and Kavli Institute at Cornell (KIC) DMREF Grant No. 1534303.

REFERENCES

[1]R. Ramesh and D. G. Schlom, Nat. Rev. Mater. **4**, 257 (2019).
[2]M. Fiebig, T. Lottermoser, D. Meier, and M. Trassin, Nat. Rev. Mater. **1**, 16046 (2016).
[3]M. A. Alam, M. Si, and P. D. Ye, Appl. Phys. Lett. **114**, 090401 (2019).
[4]J. Iniguez, P. Zubko, I. Luk'yanchuk, and A. Cano, Nat. Rev. Mater. **4**, 243 (2019).
[5]M. Hoffmann, F. P. G. Fengler, M. Herzig, T. Mittmann, B. Max, U. Schroeder, R. Negrea, P. Lucian, S. Slesazeck, and T. Mikolajick, Nature **565**, 464–467 (2019).
[6]E. A. Paisley, H. S. Craft, M. D. Losego, H. Lu, A. Gruverman, R. Collazo, Z. Sitar, and J.-P. Maria, J. Appl. Phys. **113**, 074107 (2013).
[7]Y. Chye, T. Liu, D. Li, K. Lee, D. Lederman, and T. H. Myers, Appl. Phys. Lett. **88**, 132903 (2006).
[8]H. Wu, J. Yuan, T. Peng, Y. Pan, T. Han, and C. Liu, Appl. Phys. Lett. **94**, 122904 (2009).
[9]M. H. Nam, S. C. Goo, M. D. Kim, and W. Yang, J. Phys. **187**, 012013 (2009).
[10]A. Posadas, J.-B. Yau, C. H. Ahn, J. Han, S. Gariglio, K. Johnston, K. M. Rabe, and J. B. Neaton, Appl. Phys. Lett. **87**, 171915 (2005).
[11]W. Tian, V. Vaithyanathan, D. G. Schlom, Q. Zhan, S. Y. Yang, Y. H. Chu, and R. Ramesh, Appl. Phys. Lett. **90**, 172908 (2007).
[12]A. A. Bossak, I. E. Graboy, O. Y. Gorbenko, A. R. Kaul, M. S. Kartavtseva, V. L. Svetchnikov, and H. W. Zandbergen, Chem. Mater. **16**, 1751 (2004).
[13]J. A. Mundy, C. M. Brooks, M. E. Holtz, J. A. Moyer, H. Das, A. F. Rébola, J. T. Heron, J. D. Clarkson, S. M. Disseler, Z. Liu, A. Farhan, R. Held, R. Hovden, E. Padgett, Q. Mao, H. Paik, R. Misra, L. F. Kourkoutis, E. Arenholz, A. Scholl, J. A. Borchers, W. D. Ratcliff, R. Ramesh, C. J. Fennie, P. Schiffer, D. A. Muller, and D. G. Schlom, Nature **537**, 523–527 (2016).
[14]S. M. Disseler, J. A. Borchers, C. M. Brooks, J. A. Mundy, J. A. Moyer, D. A. Hillsberry, E. L. Thies, D. A. Tenne, J. Heron, M. E. Holtz, J. D. Clarkson, G. M. Stiehl, P. Schiffer, D. A. Muller, D. G. Schlom, and W. D. Ratcliff, Phys. Rev. Lett. **114**, 217602 (2015).
[15]N. Sai, C. J. Fennie, and A. A. Demkov, Phys. Rev. Lett. **102**, 107601 (2009).
[16]W. Wang, J. A. Mundy, C. M. Brooks, J. A. Moyer, M. E. Holtz, D. A. Muller, D. G. Schlom, and W. Wu, Phys. Rev. B **95**, 134443 (2017).
[17]J. A. Moyer, R. Misra, J. A. Mundy, C. M. Brooks, J. T. Heron, D. A. Muller, D. G. Schlom, and P. Schiffer, APL Mater. **2**, 012106 (2014).
[18]D. Jena, R. Page, J. Casamento, P. Dang, J. Singhal, Z. Zhang, J. Wright, G. Khalsa, Y. Cho, and H. G. Xing, Jpn. J. Appl. Phys., Part 1 **58**, SC0801 (2019).
[19]See https://icsd.fizkarlsruhe.de/search/basic.xhtml for Inorganic Crystal Structure Database.
[20]A. J. Green, K. D. Chabak, E. R. Heller, R. C. Fitch, M. Baldini, A. Fiedler, K. Irmscher, G. Wagner, Z. Galazka, S. E. Tetlak, A. Crespo, K. Leedy, and G. H. Jessen, IEEE Electron Device Lett. **37**, 902 (2016).
[21]H. Das, A. L. Wysocki, Y. Geng, W. Wu, and C. J. Fennie, Nat. Commun. **5**, 2998 (2014).

Published under license by AIP Publishing